Dynamic Drop Testing of eVTOL Energy Storage Systems Part 2: Deformation and Post-Test Forensics Results

Justin Littell
Research Aerospace Engineer
NASA Langley Research Center
Hampton VA, 23681

Nathaniel Gardner
Research Aerospace Engineer
NASA Langley Research Center
Hampton VA, 23681

Shay Ellafrits
Research Aerospace Engineer
NASA Glenn Research Center
Cleveland OH, 44135

ABSTRACT

Researchers at the National Aeronautics and Space Administration (NASA) have conducted a series of module-level 50-ft dynamic drop tests on electric Vertical Take-off and Landing (eVTOL) Energy Storage Systems (ESS) for the generation of dynamic impact data to support standards developments. The tests were conducted on zero-state-of-charge Electric Power Systems (EPS) Electric Propulsion Ion Core (EPIC) modules at the National Institute for Aviation Research (NIAR), utilizing the NIAR outdoor drop test setup and conducted by NIAR test personnel. Four total tests were conducted on modules oriented in four different orientations. During initial post-test inspections at the drop facility, it was observed that the modules experienced varying amounts of damage in various locations and forms. The damage was quantified to the maximum extent possible via photogrammetric methods such as digital image correlation and marker tracking. Post-test modules were then disassembled, and forensics were conducted, which involved inspections into various containment structures and the cells themselves. A scoring rubric was developed in order to utilize a common methodology to quantitatively assess the damage incurred into each module as way of determining the least and most amount of damage present. Results in the form of post-test inspections, digital image correlation deformations, scoring rubric values, will be all presented, along with proposed paths forward for future work.

INTRODUCTION

Currently, there is development on a variety of non-traditional aircraft which have the potential to cause major changes to the national airspace. These aircraft, called electric Vertical Take-off and Landing (eVTOL) are comprised of new designs, materials, and operational missions. The intent of these vehicles is to provide services such as package delivery or medical supply, perform public good missions such as firefighting or disaster relief, and be able to operate like conventional taxi services by transporting people in the urban environment.

One main feature of these new types of vehicles is their ability to utilize fully or hybrid electric power systems. As with electric automobiles, the intent is to operate safely, quietly, and reliably while being able to address environmental concerns through their operation. In another parallel with electric automobiles, these electric power systems will consist of large amounts of battery modules typically containing Lithium-ion battery cells connected to onboard battery management systems, cabling, sensors and other associated hardware and are often grouped under the term “Energy Storage Systems (ESS)”.

This report is the second in a two-part series. As discussed in Part 1, there are current gaps into the certification efforts resulting from utilizing these new ESS on aircraft in the United States. Questions arise in the areas of ESS safety so these systems must be certified for operation under conditions related to safety, among many others. The certification requirements for these (and many other systems) are currently under development.

A team at NASA under the Revolutionary Vertical Lift Technology (RVLT) project has been investigating the dynamic response of ESS systems through dynamic testing. Specifically, ESS modules have been dropped from a height of 50 ft, which follows the Code of Federal Regulations Title 14 Part 27 section 952 (14 CFR § 27.952) [1] “Fuel System Crash Resistance,” test, in order to generate data for the community. The results collected from these types of tests include items such as loading levels and post-test response, which are of great interest to regulators, original equipment

Presented at the Vertical Flight Society’s 81st Annual Forum & Technology Display, May 20-22, 2025, Virginia Beach, Virginia.

manufacturers (OEMs), researchers and other interested parties.

One main goal of the research was to determine factors contributing to the response of the ESS modules. Destructive testing in the form of pinch [2], punch [3], compression [4], and bending [5] have all been studied at the cell level, and commentary on developed hazards is oftentimes provided. Two main hazards that develop from the destructive tests are thermal runaway (TR) which is where the uncontrolled cell heating leads to an explosion or fire, and Electric Shock (ES), which occurs when cell connections are broken leading to short circuits in the cell or surrounding structure. By understanding the ways at which these hazards develop at the cell level, and then conducting tests at the module level, attempts to develop a correlation between loading conditions and resulting hazards may be established.

The research plan was to utilize the 50-ft drop test as a method with multiple goals in mind. The first goal was to provide data resulting from a 50-ft drop test, and the second was to determine the performance and survivability of an ESS module subjected to a 50-ft drop test. The determination of survivability was focused on the response from the test, noting that by subjecting the module to a dynamic impact, there are factors which could create an environment suitable for hazard to occur.

Methods for determining survivability were developed by conducting post-test inspections, measurements, and ultimately post-test disassembly and forensic analysis. Ultimately, trade-offs were necessary in order to generate the required data, with a significant trade-off being the module condition necessary for post-test disassembly and forensic analysis. For the testing, the modules were in a zero-state-of-charge condition, meaning that the hazards which could develop were minimized (but not eliminated) as much as possible in the module itself. By testing at a zero-state-of-charge, a definitive commentary of the effect of TR or ES cannot be presented, only factors such as the deformations and failures in the components resulting from the tests can be conclusively identified.

In order to somewhat rectify this trade-off, a scoring rubric was developed to provide a method for quantifying the differences in test results between the tests conducted, as well as a metric for evaluation of performance. These results can then be used to guide future testing, while also providing insight and discussion on potential correlations between various loading conditions and types of damage that developed in these test articles.

The tests described herein (and in Part 1) [6] discuss results from testing from Phase 1 of the RVLT research project investigating the dynamic response of ESS systems through dynamic testing. Phase 1 specifically looked at the ESS modules themselves without additional components or structure. Phase 2, which was conducted in 2024, used the knowledge gained from Phase 1 results and expanded upon them further by conducting additional tests "within structure," which follows the spirit of the text described in [1]. Phase 3, which is expected to be completed in 2025, is intending to test a pack-level setup in an energized configuration. The details from the Phase 1 testing will now be described.

TEST DETAILS

Many of the test details are covered in Part 1 of this report [6] but will be summarized here for completeness. The modules were Electric Power Systems (EPS) EPIC Energy modules, which were ESS modules that weighed approximately 24.5 lb. and can generate 2.3 kWh of power. A picture of the module is shown in Figure 1.

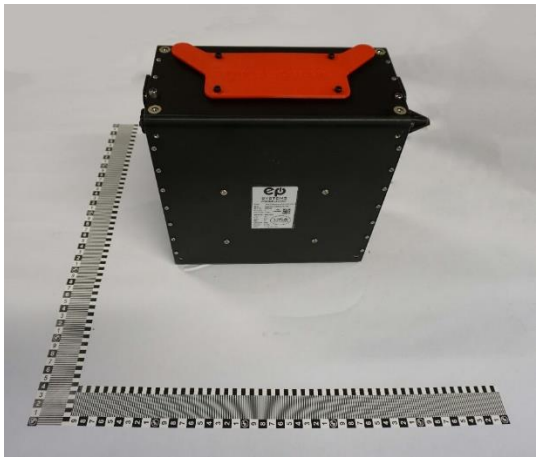

Figure 1 - EPS EPIC energy module test article

The Battery Management System (BMS), venting hardware, mid-point disconnects, or any other associated hardware was not present during this test series. Furthermore, as previously described, to protect against the threat of Thermal Runaway (TR), each module was placed into a zero-state-of-charge state. This allowed for electrical information in each cell to still be interrogated pre- and post-test, which was conducted by attaching a diagnostic monitor to the

communication port. There were also two electrode terminals on the sides. The positive electrode is on the right side of the module, while the negative electrode is on the left side (as positioned in Figure 1). In some cases, voltage was checked between these two terminals, post-test, for continuity.

All tests followed the general procedure developed in [7] and were conducted at the National Institute for Aviation Research (NIAR), utilizing the NIAR outdoor drop test setup and conducted by NIAR personnel. For each test, the module was dropped from a height of 50 feet while connected to a guided trolley which is the setup NIAR has used for previous ESS testing [8]. Data collected from the tests was in the form of temperatures, accelerations and digital image correlation measurements, which were used to determine a quantitative time history, to the best extent possible, of the deformation that occurred during the impact event. The digital image correlation data were acquired from two systems, a global and a local, which were imaging two sides of the test articles. There were several factors which limited the specific sides that could be speckle coated, which were constraints on both the test setup in the bunker as far as cable runs and sun position, along with the constraints derived from the orientation of the test articles at impact. Thus, while two of the sides were painted, these two sides may not have been the two that experienced the largest amounts of deformation. Additionally, the local system was the main system used for deformation tracking in the test articles during impact. The global system was mainly focused on obtaining impact conditions and overall kinematics of the test article during the tests, which was accomplished through marker tracking. A picture of the test setup is shown in Figure 2.

Figure 2 - NIAR test setup

An example of the speckle coating used for digital image correlation is shown in Figure 3 for the Sideways orientation test article. The left facing surface is the bottom face of the Enclosure Assembly representing the bottom of the test article, which is painted with the local speckle pattern. The right facing surface represents the side of the Enclosure Assembly, which contains the identification placard and is painted with the global speckle pattern.

Figure 3 - Speckle coatings on Sideways test article for use with digital image correlation

Post-test, the general test procedure required for the modules to be actively monitored for a period of 1 hour immediately following the impact. During this hour, attention was primarily given to ensuring temperatures were stable and thermal runaway (TR) was not occurring. Methods used to determine this were to monitor the module enclosure temperature, look for visual signs of smoke or fire, and detect the presence of an electrolyte smell. If it was determined no TR was occurring, the test article was approached, and visual inspections began. After the visual inspections, the test article was placed in outdoor storage for passive monitoring for a period of 24 hours. Once it was determined that the test article was stable after the 24-hour period, the test article was ready for tear down and forensic inspections.

The post-test teardowns and forensics for Flatwise, Rightside Up and Upside Down test articles occurred on January 22nd and 23rd, 2024, while the forensics for Sideways test article occurred on April 10th, 2024. The modules were carefully disassembled with care being

taken to not further disturb the potentially damaged components.

SCORING RUBRIC DEVELOPMENT

The modules were scored using a scoring rubric which was developed to provide a quantitative result of the damage seen during the tests. The rubric contained two levels of grading - the first at the assembly level and the second at the cell level. The assembly level examined the three major systems that acted as containers around the internal cells: the Enclosure Assembly, the Containment Assembly, and the Cell Assembly. This level of grading scored each test article, with severity grades of 1 – low, to 4 – severe, based on inspections conducted in each of the assemblies after each test. Ratings were based on a combination of comparative analysis between the various test articles, but also total severity (i.e. two modules can have the same rating). There were then multipliers placed on those results, with the Cell Assembly having a multiplier of three since it was the first line of defense for TR containment, with reduced multipliers being used when moving further away from the cells themselves. The assembly level rubric is shown in Table 1.

Table 1 - Assembly Level Rubric

Assembly	Severity	Multiplier	Notes
Enclosure	Low (1) Medium (2) High (3) Severe (4)	1	
Containment	Low (1) Medium (2) High (3) Severe (4)	2	
Cell	Low (1) Medium (2) High (3) Severe (4)	3	

The second part of the rubric was at the cell level. At the cell level, the focus was on the cell damage and quantifiable metrics were developed in five different categories, which represented five different types of events seen at the cell level and rated for both *type* and *amount* of damage seen. The cells were examined for: 1 – Pouch Puncture, 2 – Pouch Breach, 3 – Pouch Deformation, 4 – Electrical Shorting and 5 – Presence of Electrolyte Smell. Pouch puncture and breach were primarily determined by visual inspection. Electrical shorting was determined by examining voltage continuity via the use of a multimeter. The presence of electrolyte was determined by smell. Pouch puncture differed from pouch breach in that a puncture is the result of a third-party object (such as a standoff) affecting the integrity of the pouch structure whereas a pouch breach is the result of a body or inertial load from the pouch itself. The differentiation between the two were primarily determined by visual inspections. Actual numbers were counted and recorded in the rubric, along with notes of interest, should there be any. The multipliers on the type of damage were based on the severity of the type of damage and it's expected contribution to TR. So, both types of failures in the pouch cell – puncture and breach - were scored much higher than pouch deformation and shorting since a pouch failure was almost necessary for a TR event to occur. The electrolyte smell grade was similar. While this was only a binary yes/no, the presence of an electrolyte smell was further evidence of pouch failure. Notes on the relative severity of the presence of electrolyte were also recorded in the notes section. The cell level damage rubric is shown in Table 2.

Table 2 - Cell Level Rubric

Damage	Number of Cells	Multiplier	Notes
Pouch Puncture		10	
Pouch Breech		10	
Pouch Deformation		4	
Electrical Shorts		3	
Electrolyte Smell (Y/N)		10	

After the forensics for each module was completed, the results of the assembly level and cell level scores

from the tests were summed, and the module scores were compared to determine the most and least severe damage in the modules. The results from the scoring rubric were compiled during the post-test inspections and will be presented later in this report.

RESULTS

Flatwise Orientation

For the Flatwise orientation test, the test article was placed such that the top vent facing perpendicular to the impact surface, and oriented such that the vent port was facing South, and the positive electrode was facing West. The test was conducted on November 14, 2023 at 12:32 PM local time. The outside temperature was 68.3° F with a relative humidity of 35.6%. Winds were 6 miles per hour (MPH) gusting to 10 MPH. The test article impacted at the north-west corner, with a north-side low angle of 17.9 degrees, west-side low angle of 1.4 degrees and an impact velocity of 46.9 feet per second (ft/s). After the 1-hour post-test monitoring, there was no sign of spark, smoke or presence of electrolyte, so it was assumed that TR was not occurring, and post-test inspections began.

During post-test inspections, the test article showed noticeable signs of permanent deformation at both the north side and south side impact edges. There was some inward deformation of the top surface indicating the motion of the internal components pulling the enclosure downward during the test. The post-test orientation of the test article is shown in Figure 4.

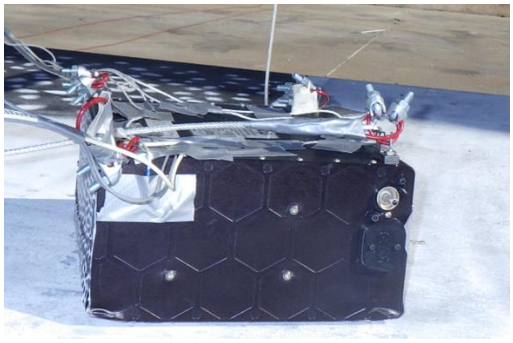

Figure 4 – Flatwise end view, post-test

The north side is on the left side of Figure 4, while the south side is on the right. Large indentations are present in the north and south side edges, due to the nature of the impact. In addition, the four fasteners attaching the Enclosure Assembly to the Containment Assembly all ended up slanted downward, indicating that inside mass has shifted downward relative to the Enclosure Assembly. The top face, which was the face containing the vent port was slightly bowed inward and the bottom face, which was the face oriented toward the impact was slightly bowed outward. It appeared the rotation through the impact may have shifted the internal components toward the bottom face, which would cause the observed deformation in the enclosure. The upper face of the test article is shown in Figure 5, with the vent port in the foreground.

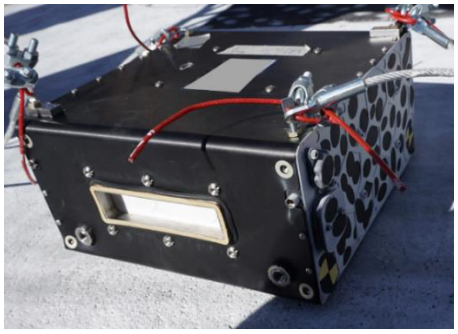

Figure 5 - Flatwise top view, post-test

The deformation results from the digital image correlation measurements are presented next. The local system was focused on the bottom face of the test article. The results from vertical and out-of-plane deformations during test article maximum deformation and permanent deformation are shown in Figure 6.

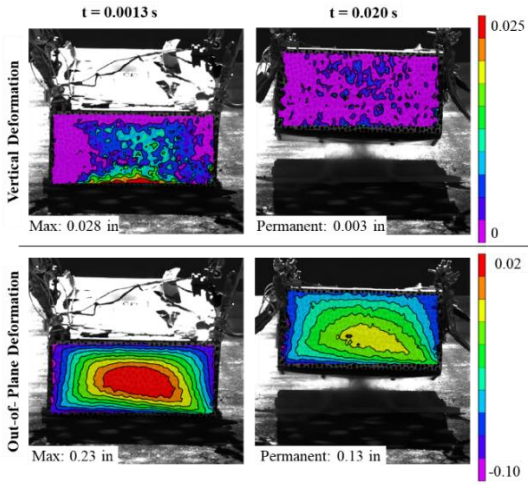

Figure 6 - Flatwise digital image correlation results

The maximum vertical deformation in the test article was approximately 0.025 inches, which occurred at the

time of the initial impact and first peak in the acceleration response. The deformation was computed through the entire impact, and a post-impact time at 0.02 s shows negligible permanent vertical deformation. The out-of-plane deformation exhibited a large outward displacement at time of maximum accelerations. Since this was the bottom face of the enclosure, there were no attachments to the inner structure. This feature caused this motion to depict typical behavior of an unsupported flat face, with oscillation modes cycling between outward and inward motion. The outward permanent deformation post-impact ended up at approximately 0.13 inches. Due to the constraints in the test, the face observed in the digital image correlation data was the bottom face and thus only limited commentary on the compression of the internal component can be given, which would have resulted from the oscillation in the out-of-plane deformation. With this in mind, the module was disassembled, and the internal enclosures and individual cells were examined.

While there was some deformation in the corners of the module due to the off-nominal impact and rotation through the impact sequence, the components near the top of the module associated with the electrode connections appeared to be relevantly undamaged. Readings were collected indicating that shorts in the electrical components were not present. The electrode terminals of the battery did not show damage that would cause the cells to short against the enclosure. Once those observations were completed, the Enclosure Assembly was removed.

The internal module components exhibited convex bowing deformation toward the impact surface side. However, the deformation did not result in any shorting, either from the cells to the enclosure or to each other. Once the Containment and Cell Assemblies were completely disassembled and removed, there was a slight electrolyte smell present, indicating potential damage somewhere. The cells were then inspected to determine if visible damage had occurred. A bottom view of the cells is next shown in Figure 7.

Figure 7 - Flatwise, pouch cell view. Impact side up

All cells received damage due to the drop test. Ten cells exhibited permanent deformation from the standoffs protruding into the sides of the cells, which is noted by the circular indentations in each quadrant approximately 2 inches away from the edges (not shown). In addition, 20 cells received indentations on the non-impact side due to the residual impact of the potting compound and casing contacting the cells during the impact. All 30 cells buckled on the impact side, which is shown in Figure 7, noting the impact side is facing upward. The buckling is evident from the creases and localized deformations in the cells, which were a direct result of the impact.

In summary, at the assembly level, there was minimal deformation, but no damage to the enclosure, slight electrolyte smell at the containment and punctures due to the standoffs and bowing in the cells. The scoring was graded as Low for the Enclosure, Medium for the Containment, and Medium for the Cell Assemblies, respectively. At the cell level, there were zero puncture or breach failures visible, however all 30 cells were deformed and there was an electrolyte smell present. The assembly level damage score was 11 and the cell level damage score was 130, resulting in a total score of 141. Next the Rightside Up orientation was examined.

Rightside Up Orientation

The Rightside Up orientation positioned the test article with the vent facing upward and opposite of the impact surface and oriented the test article such that the positive electrode was facing West. The test was conducted on November 14, 2023 at 3:26 PM local time. The outside temperature was 68.2° F with a relative humidity of 34.8 %. Winds were 5.7 MPH gusting to 12.3 MPH. The test article impacted at the south-east corner, with a south-side low angle of 2.2

degrees, east-side low angle of 2.6 degrees and an impact velocity of 52.8 feet per second (ft/s). There was no sign of spark, smoke or presence of electrolyte, so after the hour of monitoring was over, post-test inspections began.

Inspections revealed some bulging in the sidewalls of the Enclosure Assembly near the bottom which contacted the impact surface. The bottom face of the test article which contacted the impact surface appeared to be relatively undeformed, likely due to the close-to-nominal impact angle. The bulging, which was an indication of the internal components shifting downward toward the bottom face of the module, was present on all four sides. This result is further supported by the orientation change of the fasteners on the sidewalls of the enclosure. All fasteners have shifted to be oriented downward, again suggesting the internal components shifted. The top surface of the module, which was on the opposite of the impact, experienced inward or concave shaped deformation. A post-test view of the test article is shown in Figure 8.

Figure 8 – Rightside Up end view, post-test

The bottom face that contacted the impact surface is to the left in Figure 8. The sidewalls near the bottom face are where there was considerable deformation present. The four fasteners (three visible, one covered with tape) are oriented to the left, which is the downward direction toward the impact. The digital image correlation data was next examined to determine the effect of the downward shift from the internal components. The digital image correlation data is shown next in Figure 9.

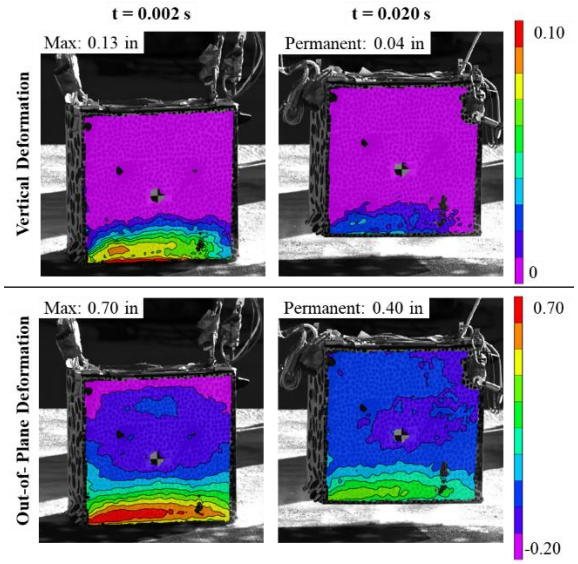

Figure 9 – Rightside Up digital image correlation results

The crushing of the bottom portion of the Enclosure Assembly was clearly captured in the digital image correlation data. The crushing was measured in both the vertical and out-of-plane directions and showed maximum values of 0.13 inches for the vertical direction and 0.70 inches in the out-of-plane direction. The vertical crush was expected to cause compression in the longitudinal direction in the pouch cells. However, since digital image correlation was measuring Enclosure Assembly deformation only, the internal pouch cells were not necessarily expected to crush with similar magnitude since there were still additional structure present within the module.

Another item that the digital image correlation data depicted was that deformation was limited to the lower third of the test article. The upper two-thirds of the test article did not experience any significant deformation from the test, which can be noted by examining the color plots in the permanent column on the right. Thus, the assumptions going into the disassembly were involved around seeing the amount (if any) of crush within the pouch cells themselves. With these results in mind, the module was disassembled, and the internal components were examined.

Since the electrode connections were on the opposite side of the impact surface, there was minimal to no deformation in these components. As a result of this lack of deformation, no shorts were measured on the connections to the enclosure, and connectivity remained for post-test diagnostics. However, the

Containment Assembly revealed the change in orientation in the standoffs. The fastener orientation change observed post-test was a result of downward rotation of the four standoffs on each of the enclosure sides. This rotation is not seen in the digital image correlation results because those results only measured the relative position of the standoffs with relation to the Enclosure Assembly, which did not change. This result meant that the behavior on the standoffs was rotational only, and not positional, and mainly due to the relative motion between the Enclosure Assembly and the internal components. The change in orientation is noted in Figure 10, where the Enclosure Assembly has been removed revealing the Containment Assembly.

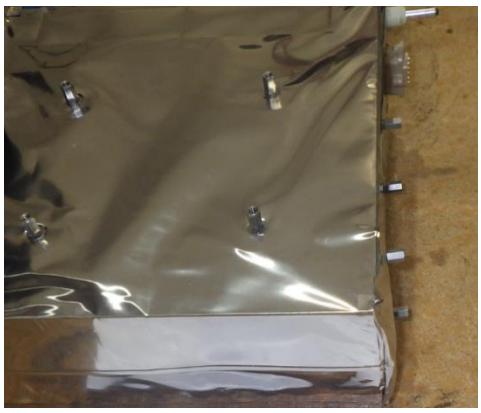

Figure 10 - Rightside up Containment Assembly

The standoffs changed orientation, however because they were not directly on the side of the impact, they did not cause tears in the Containment Assembly, which is the silver object shown in Figure 10. This result offered evidence that the internal pouch cells would be unaffected by the standoff change in orientation. The Containment and Cell Assemblies were next removed in order to reach the cells. The cells are shown next in Figure 11.

Figure 11 - Rightside up pouch cells. Side view, impact side down

The major type of deformation observed from the examination of the cells was the compressive crushing, which occurred on the impact side which is shown at the bottom of Figure 11. The compression was revealed by noting the rippling in the modules themselves. The deformation was more pronounced in the middle of the module than on the ends, due to the middle being unsupported by the rigidity of the Enclosure Assembly. This trend also followed the contour plots presented from the digital image correlation data in Figure 9, and suggests the digital image correlation data provided evidence of the internal cell motion using the Enclosure Assembly as a surrogate. When examining the cells themselves, there were no discernable breaches of the cells in this orientation, and there was only a very faint electrolyte smell detected.

In summary, at the assembly level, there was some deformation in the Enclosure Assembly, little to no damage in the Containment Assembly but there was minor deformation in the Cell Assembly. The scoring was graded as Medium for the Enclosure, Low for the Containment, and Low for the Cell Assemblies, respectively. At the cell level, there were zero puncture or breach failures visible, however all 30 cells were deformed and there was a faint electrolyte smell present. The score for the assembly level damage was 7 and the score for the cell level damage was 130, giving a total score of 137. Next the Upside Down orientation was examined.

Upside Down Orientation

The test article in the Upside Down orientation was configured with the vent facing downward toward the impact surface and oriented such that the positive electrode was facing East. The test was conducted on November 13, 2023, at 4:41 PM local time. The outside temperature was 69.6° F with a relative humidity of 40.7 %. Winds were 4.3 MPH. The test article impacted at the north-west corner, with a north-side low angle of 6.2 degrees, west-side low angle of 2.3 degrees and an impact velocity of 48.5 feet per second (ft/s). There was no sign of spark, smoke, or presence of electrolyte, so after the hour of monitoring was over, post-test inspections began. A post-test configuration of the test article is shown in Figure 12 and Figure 13.

Figure 12 - Upside Down chiller plate side view, post-test

The two sides of the test article were not symmetric due to the presence of an internal chiller plate being located inside the enclosure on the side opposite of the electrodes and placard. This plate ran along the entire side of the module and was present to keep the modules cool during normal operations. While the chiller plate was not connected during the test series, it's presence within the enclosure led to non-uniformity in overall module stiffness between the two sides which ultimately led to non-uniformities in some of the deformations observed in some of the orientations tested. The chiller plate side is shown above in Figure 12, while the opposite side is shown in Figure 13

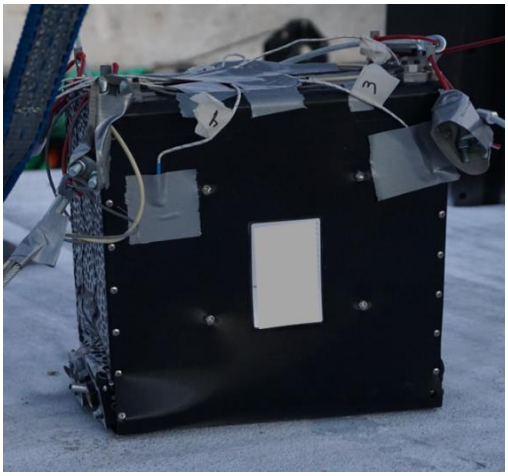

Figure 13 - Upside Down placard side view, post-test

The test article enclosure experienced large amounts of deformations on the locations closest to the impact face. Significant amounts of bulging are present at the bottom corners; however, the bulging is not symmetric between the two sides due to the presence of the chiller plate. The side opposite of the chiller plate, which is shown in Figure 13, experienced a greater amount of deformation which caused the test article to "lean" in that direction. However, on both sides, the small fasteners at the enclosure edges on the impact side failed due to the bulging of the enclosure, which caused the enclosure to separate at these locations. This type of failure is shown in Figure 14.

Figure 14 - Upside down corner fastener failure

The failure in the fasteners in the corner can be observed in the upper left portion of the image in Figure 14. These fasteners connected the part of the enclosure impacting the impact surface. The bulging, due to the shift in the internal components, resulted in the fastener failure. As seen in the test data from drops in other orientations, the fasteners attached to the standoffs located in the middle of each of the sides changed orientation, suggesting shifting of the internal components toward the impact face. The digital image correlation data was next examined and is shown in Figure 15.

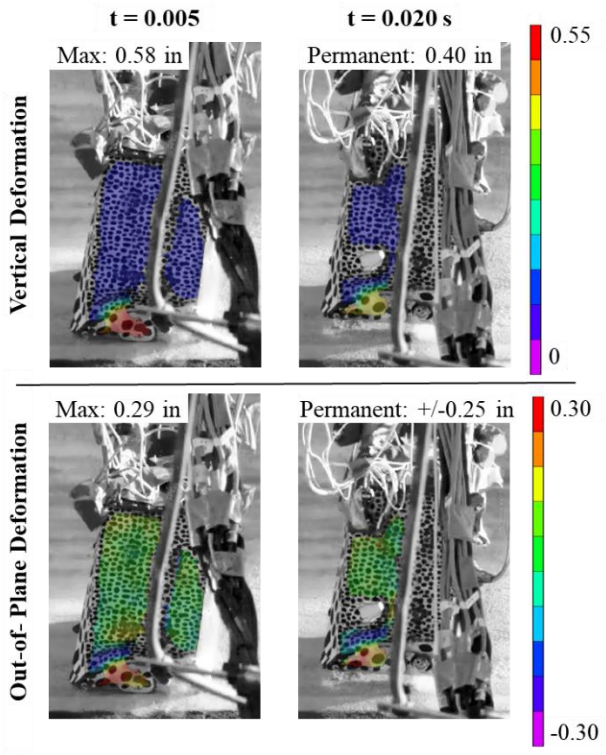

Figure 15 - Upside Down digital image correlation results

Digital image correlation results provided a quantitative measurement of the deformation that occurred in the module from the positive electrode end face. The view is partially obstructed due to the data cabling entering the foreground of the camera view, but still provides insight into the module deformation as a whole. The uneven crush deformation caused the test article to lean toward the right, which was toward the placard face, and opposite of the chiller plate. The two images on the left of the fixture represent the test article at 5 ms after initial impact, which was after the initial peak values of acceleration occurred from the corners impacting the surface. Peak vertical deformation was in the range of 0.58 inches, while peak out-of-plane deformation was approximately 0.29 inches bulging outward. The permanent deformations were slightly less, showing 0.4 inches in the vertical direction and 0.25 inches in the out-of-plane direction and present in the test article after the primary loading event occurred. As with the other results, the deformation was localized primarily in the portion of the test article nearest the face contacting the impact surface.

During the initial inspection of this module, there was an electrolyte smell present and there were signs of internal shorting within the module. During the post-test tear downs and forensics inspections, due to the large deformations observed during the post-test inspections, extra care was required to remove the Enclosure Assembly in an attempt to not disturb the internal components further. The Enclosure Assembly was successfully removed without further damage occurring, and after the Enclosure Assembly was removed, the Containment Assembly was examined. The Containment Assembly is shown in Figure 16.

Figure 16 - Upside Down Containment Assembly, standoffs bent, metal breached

The Containment Assembly showed significant damage. The standoffs were not only rotated in their orientation, but significantly bent which caused tears at multiple locations within the assembly. In addition, it was observed that the standoff damage resulted in a breach of one of the end pouch cells. It is likely that the electrolyte smell that was detected was due to these breaches. Before the Containment Assembly was

removed to reveal the Cell Assembly, the upper portion of the modules containing the terminals, busbars and circuit board was examined. The area around the positive electrode side is shown Figure 17.

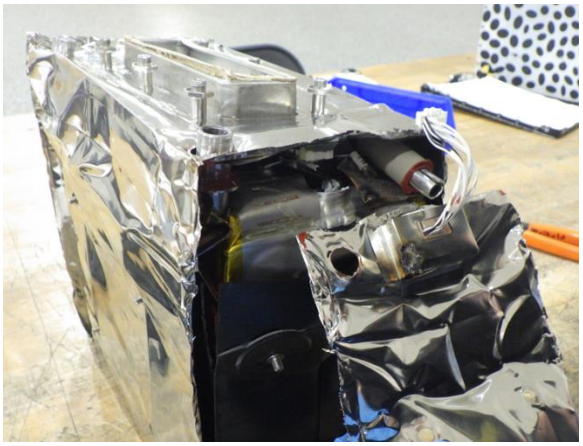

Figure 17 - Upside Down positive electrode area

There were numerous electrical shorts observed in the test article. Connectivity checks revealed shorts between five of the cells to the enclosure chassis, along with a short from three of the virtual cells. The shorting damage which occurred on the inner interface of the communication connector is shown in Figure 17, noting the charred area below the white wires. The shorts were much more evident on this configuration since the impact pushed the top of the busbar and other components which are normally above the cells, inward toward the cells, compressing many of the upper connection points. The busbar assembly caused indentations into the top of two cells, exposing the electrodes of the cells. The cells themselves were the last items inspected. An image of the cell inspection is shown in Figure 18.

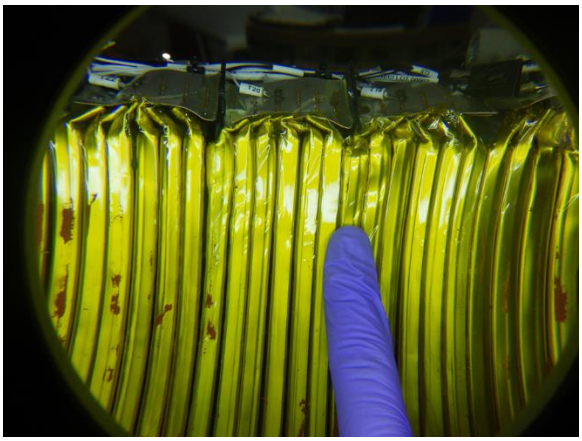

Figure 18 - Upside Down pouch puncture

In summary, at the assembly level, there was significant damage in the Enclosure Assembly, multiple tears in the Containment Assembly, and several electrical shorts due to the busbar intrusion in the Cell Assembly. The scoring was graded as High for the Enclosure, High for the Containment, and High for the Cell Assemblies. At the cell level, there were five cell punctures, no cell breaches, deformation on 9 cells, with 17 electrical shorts and a strong electrolyte smell present. The assembly level damage score was 18, while the cell damage score was 147, resulting in a total score of 165.

Sideways Orientation

The Sideways orientation test was conducted on March 13, 2024, at 9:07 am local time. It was not conducted at the same time as the others due to availability of the module. However, the test setup which included the lifting configuration, instrumentation and test conduct were identical to the others. The Sideways orientation positioned the side with the positive electrode facing the impact surface and oriented it with the vent tube facing North. The outside temperature was 53.9° F, the wind was calm and relative humidity was 61.5%. The test article impacted flatwise along the west edge, with a west-side low angle of 6.5 degrees and an impact velocity of 50.6 feet per second (ft/s). Post-test, there was no sign of spark, smoke, or presence of electrolyte, so after the hour of monitoring was over, post-test inspections began. A post-test orientation of the test article is shown in Figure 19.

Figure 19 - Sideways post-test

Post-test inspections revealed many of the characteristic deformations seen in the other tests. There was enclosure deformation, mainly in the warping of the side wall opposite of the chiller plate, near the impact location. The sidewall with the chiller plate did not experience any visible deformation. The end opposite of the impact surface experienced inward deformation due to the internal components pulling away during the impact. A review of the high-speed video during the impact sequence revealed a visible spark exiting the negative electrode for a brief moment. This observation provided a high level of confidence that an electrical short had occurred during the sequence, however, there were no visible sparks that occurred post-test. The deformation from the local digital image correlation system, imaging the bottom face of the enclosure, is next shown in Figure 20.

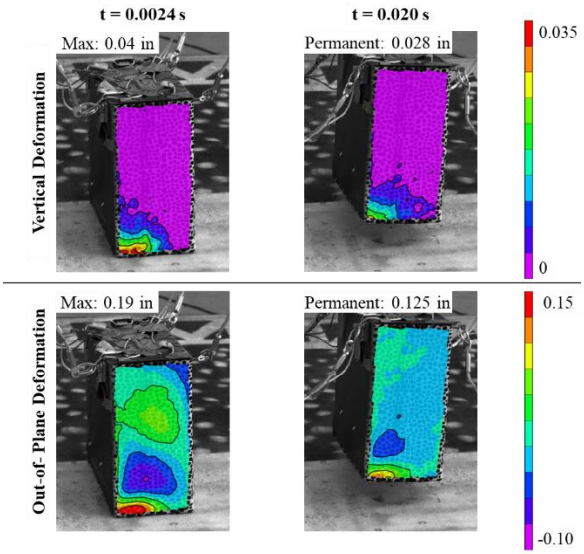

Figure 20 - Sideways digital image correlation results

The digital image correlation results provided a quantitative assessment of the local deformation which occurred in the test article during impact. The side with the chiller plate was orientated on the right side of the test article in the images in Figure 20, and the results show that there was almost no deformation in either the vertical or out-of-plane directions on this side. In contrast, the side opposite of the chiller plate experienced significant deformations in both directions measured. The maximum and permanent vertical deformation was 0.04 and 0.028 inches respectively, while the out-of-plane deformation was an order of magnitude higher, at 0.19 and 0.125 inches for the maximum and permanent values, respectively. The digital image correlation data confirmed the visual inspection results of an asymmetric deformation behavior in the impact facing side. With the knowledge gained from the digital image correlation, the module was disassembled for post-test forensics.

During the initial inspection of this module at the test site, there was an electrolyte smell present along with the previously described signs of internal shorting within the module. During the post-test tear downs and forensics inspections, the extent of the damage was revealed. There was significant rotation in orientation in the standoffs between the enclosure and the Containment Assembly on the sides. In the standoffs located on the downward facing end, there was significant movement of the standoffs inward toward the cells themselves. The shift in the standoffs for both faces is shown in Figure 21.

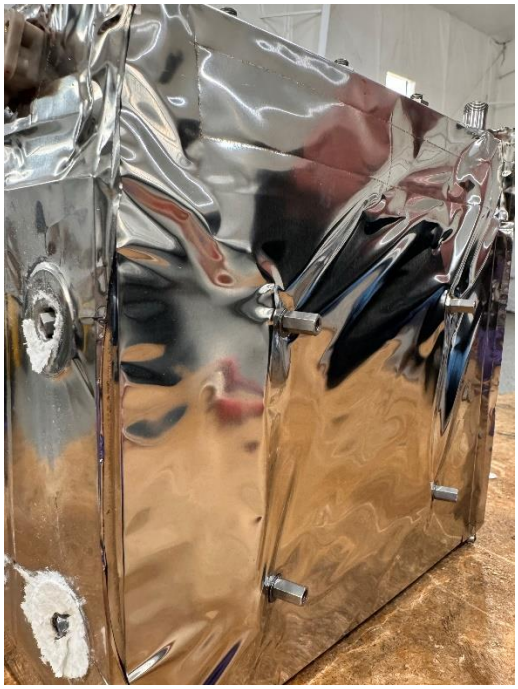

Figure 21 - Sideways standoff orientation shift. End face on left, side face on right

The standoffs on the end face appeared to disappear into the Containment Assembly. However, further inspections reveal they compressed into the Cell Assembly and into the cells themselves, as shown in the Cell Assembly in Figure 22.

Figure 22 - Sideways Cell Assembly

The Cell Assembly had multiple cracks at the standoff interfaces. The most severe cracks were in the lower left standoff, which penetrated directly into the pouch cell itself. The removal of the Containment Assembly revealed multiple instances of charring. An example of this on the positive electrode is shown in Figure 23.

Figure 23 – Sideways negative electrode charring

Since the sideways orientation placed the electrode on the end face contacting the impact surface, upon contact, the electrode pushed inward, creating a short in the Containment Assembly. In addition to this short, the inward motion of the electrode also caused significant damage to four busbars. Finally, the cells themselves were examined. A bottom view of the cells is shown in Figure 24 .

Figure 24 - Sideways pouch cells

Once the cells were isolated, there was a strong odor of electrolyte present. There was deformation in all the cells, which were shifted toward the impact end (to the right), as shown in Figure 24. Additional breaches

were noted in the cells themselves, and all cells experienced both a shearing shift in the lateral direction and a bending in the upper ¼ position of the cells.

There was notable swelling of 3 cells on the impact side where the standoffs breached the cells. It was concluded that the 3 cells that showed signs of swelling were all breached by the standoff, and the swelling being the result of the cell losing compression from the vacuum sealing process. This hypothesis was confirmed with the cells having a measured voltage ranging from 0.6 mV to 2.2mV, essentially proving that the cells were dead.

In summary, at the assembly level, there was moderate damage in the Enclosure Assembly, multiple tears in the Containment Assembly, and several electrical shorts due to the standoff intrusion in the Cell Assembly. The scoring was graded as Medium for the Enclosure, High for the Containment, and Severe for the Cell Assemblies, respectively. At the cell level, there were three cell punctures, three cell breaches, deformation in all cells, with 15 electrical shorts and a strong electrolyte smell present. The score for the assembly level damage was 20, while the score for the cell damage was 235, giving a total score 255.

RUBRIC RESULT SUMMARY

After all inspections were completed the results from the rubrics were compiled, with the full results being shown in Table 3.

Table 3 - Rubric Scores

Orientation	Assembly level damage	Cell level damage	Total
Flatwise	11	130	141
Rightside Up	7	130	137
Upside Down	18	147	165
Sideways	20	235	255

There appeared to be a natural division between the four tests, with the score of 150 being the division line. The Flatwise and Rightside Up tests were the two tests which fell below the 150-division line, and it should be noted these were the two modules in which post-test diagnostic measurements for voltage and temperatures were able to be measured. Thus, the score aligns with the assumptions of the damage made by conducting the post-test diagnostic measurements. The two tests above the 150-division line were the Upside Down and the Sideways, which appeared to have significantly more internal damage both in the cell deformations, breaches and internal shorting.

The sideways orientation produced the highest score, most of which was generated from higher scores at the cell level. There were multiple points of damage within these cells, both experiencing breaches due to standoff puncturing and shifting/shearing due the cells being in a sideways orientation.

As presented in Part 1, generally all accelerations for all of the tests were high and all magnitudes and durations were in the same general range. From Part 1, peak accelerations as measured by the middle accelerometer were 1,286 g, 1,498 g, 743 g and 1,463 g for the Flatwise, Rightside Up, Upside Down and Sideways tests, respectively. The acceleration levels do not correlate with the final rubric scores. Noting these results, it appears the primary driver of the differences in the damage seen was the orientation of the modules in the tests.

The digital image correlation data provided valuable insight into the behavior into the internal components and was a valuable tool to use. While it was limited in some cases due to test and orientation constraints, and could not directly measure cell motion within the module, the data did provide evidence into the response of the Enclosure Assembly at specific orientations for the tests. Digital image correlation will continue to be implemented in all future testing to gather critical data and provide insight into the full-field response of the test articles.

DISCUSSION

A series of four tests were conducted on zero-state-of-charge EPIC ESS modules for the investigations of ESS module response. Loading conditions were identified, and factors contributing to the various types and locations of failures has been presented.

Two of the orientations produced lower levels of damage which allowed for post-test continuity in the cells to be present. Two of the orientations had greater

damage and post-test continuity in the cells was unable to be performed. After all testing was complete and the scores compiled, general trends showed the items which directly affect the cell integrity were the main factors driving the levels recorded in the scoring rubric, with the highest measured scores directly reflecting the increased levels of damage in the modules.

One thing that has not been presented is the commentary involving likelihood of TR or other hazards due to the damage and deformation obtained from the tests. This has been purposely omitted since definitive statements and/or conclusions on these hazards cannot be made due to the modules zero-state-of-charge status. While there are quantitative results which can potentially be used to infer results from charged modules, these types of extrapolations will not be made.

Furthermore, the effect of the results presented on a hypothetical aircraft will also not be presented since the tests are not in an aircraft structure, and the modules being tested are without external connections or monitoring systems which could be used to prevent the initiation and spread of TR or other hazards using the control systems or other logic built utilizing additional ESS installed hardware.

This data gathered and presented was used to define the conditions for Phase 2 of the research which better simulated an "installed condition" for a generic vehicle design. Several more zero-state-of-charge modules were tested from a 50-ft height, but utilized attenuation systems to limit the input acceleration to either 80 g or 220 g. The decision to use accelerations as input loads, along with the prescribed height of 50 feet, is based on several factors.

In general, for conducting research associated with 14 CFR § 27.952 50-ft drop test regulation, there are several factors which need to be considered. The first is the requirement of 50 ft. This requirement essentially fixes the amount of kinetic energy present in the system/test article at impact, assuming the system/test article weight is defined and known. However, this leaves no guidance on acceleration levels other than the impact surface must be rigid. In contrast, the certification criteria in other components such as the rotorcraft seats [9] are defined by both velocity (which can be converted into kinetic energy) *and* acceleration levels. Thus, input conditions are fully covered in the requirements.

Taking these factors a step further, more differences arise when attempting to correlate loading environments to data collected from full scale crash testing. For example, in a recent Lift+Cruise (L+C) test conducted at NASA Langley Research Center in 2022 [10], the loading environment was established through defined/fixed impact velocities with acceleration responses resulting from the measurement locations from the aircraft test article.

These factors were considered when the Phase 2 test Plan was developed. The chosen impact conditions were a mix of both requirements and vehicle test data. Thus, the requirement of a 50 ft drop height was used in conjunction with an attenuation system developed to simulate the 2022 L+C test. The L+C test conditions included velocities that were less than what is developed from the 50-ft test but simulated the ESS modules "within structure" as the installed condition utilizing (idealized) actual acceleration response pulse magnitudes and durations. It was determined to test to the rule, but provide a realistic input pulse, which simulates, to the best extent possible, an installed condition in an eVTOL vehicle based on real test data. While Phase 2 will also not be certification tests of ESS modules, it is hoped that the data generated will be ultimately used to provoke discussion in the community such that the most applicable test requirements can be developed. These requirements can then pave the way toward widespread eVTOL adaptation and usage.

AUTHOR CONTACT

Justin Littell - Justin.D.Littell@nasa.gov

Nathaniel Gardner - Nathaniel.W.Gardner@nasa.gov

Shay Ellafrits - Shay.A.Ellafrits@nasa.gov

ACKNOWLEDGEMENTS

The authors would like to thank Rob Huculak and his test team at NIAR for conducting the 4 drop tests. In addition, the authors would like to thank Joseph James, Spencer Wright, Derek Larsen and at Brad Mowry at EPS for the support and guidance on the ESS module technical data and for assisting in post-test forensic inspections.
.

REFERENCES

1. Code of Federal Regulations. "Fuel System Crash Resistance." 27 CFR §27.952. October 3, 1994.

2. F. Ren, T. Cox and H. Wang. Thermal Runaway Risk Evaluation of Li-ion Cells Using a Pinch-Torsion Test. Journal of Power Sources, Volume 249, pp. 156-162, 2014

3. H. Luo, Y. Xia and Q. Zhou. Mechanical Damage in a Lithium-ion Pouch Cell Under Indentation Loads. Journal of Power Sources, Volume 357, pp. 61-70, 2017.

4. S. H. Chung, T. Tancogne-Dejean, J. Zhu, H. Luo, T. Wierzbicki. Failure in Lithium-ion Batteries Under Transverse Indentation Loading. Journal of Power Sources, Volume 389, pp. 148-159, 2018.

5. J. K. Strak Goodman, J. T. Miller, S. Kreuzer, J. Forman, S. Wi, J. Choi, B. Oh and K. White. Lithium-ion Cell Response to Mechanical Abuse: Three-point Bend. Journal of Energy Storage, Volume 28, 101244, 2020.

6. Littell, J.D., Gardner, N.W., and Ellafrits, S.A. "Dynamic Drop Testing of eVTOL Energy Storage Systems Part 1: Drop Test Data Summary."" Proceedings from the Vertical Flight Society 81st Annual Forum. May 20-22, 2025. Virginia Beach, VA.

7. Littell, J.D., Gardner, N.W., and Ellafrits, S.A. "Dynamic Testing of eVTOL Energy Storage Systems: Literature Review and Path Forward." NASA TM 20220015117. January 2023.

8. NIAR-WSU. "NIAR conducts 50-ft eVTOL battery drop test per 14 CFR § 27.952." December 2, 2022. https://www.wichita.edu/industry_and_defense/NIAR/MediaCenter/2022-12-22.php. Accessed March 28, 2024.

9. Federal Aviation Administration. "Emergency Landing Dynamic Conditions." 14 CFR § 27.562. Amended November 13, 1989.

10. Littell, J.D. and Putnam, J.B. "A Summary of Test Results from a NASA Lift + Cruise eVTOL Crash Test." Proceedings from the Vertical Flight Society's 70th Annual Forum. West Palm Bean, FL. May 16-18, 2023.